

Signal Processing Final Project: Use filter processing to efficiently synthesize seismic simulation waveforms

Xxx Xxx^{1*}

¹Department of Earth Sciences, University of Oregon, USA

Key Points: Based on the basis waveform function, the filter approach is more efficient to synthesize seismic waveforms

Abstract

In general, seismic simulation takes convolution of Green's function and rise time function to produce synthetic waveforms. A fine earthquake simulation takes a lot of computing time, and in forward modeling the rise time function is very various and tricky. This project presents an approach to generate synthetic waveforms by the filtering the basis synthetic waveforms. This allows synthetic waveforms to flexibly change rise time function to meet different requirements of rise time combination. In addition, this filter approach significantly saves computing time.

Plain Language Summary

Earthquake rupture time is one of keys for seismic simulation. However, earthquake rupture time is various, so the problem is how to efficiently simulate seismic waveforms with different rupture times. Here, I use a filter approach and high frequency (short rupture time) synthetic seismic waveforms to generate lower frequency (longer rupture time) synthetic waveforms. The results show lower frequency synthetic waveforms perfectly match the waveforms from seismic simulation and this approach is able to save more computing time.

Introduction

Earthquake scenario simulation is an approach to understand the feature of seismic wave propagation and the potential seismic hazards. Lee et al. (2008, 2009, 2015) used seismic simulation to investigate the effects of tomography and velocity structure. Lee et al. (2015) used spatial stochastic model to simulate the near-source ground motion for predicting ground motion. The seismic simulation with a fine velocity model will take a lot of time to compute (Lee et al., 2015), so how to save the computing time is critical. Moreover, the rise time function observed by real events is various (Melgar & Hayes, 2017) and its shape wouldn't be described by a single function (Kubo et al, 2017). This also increases the variances in earthquake scenario

simulation. In this project, the goal is to make seismic simulation be more flexible to change the rise time function, respond to different scenarios and save more computing time. I use a suitable filter to generate the filtered synthetic wave based on the basis waveform function instead of re-simulation for different rise times.

Method

There are two components: 1. forward simulation of seismic waveforms. 2. using filter to generate filtered synthetic waveforms. The forward simulation of seismic waveforms uses the open-source MudPy code (Melgar and Bock, 2015) with 1-D layered velocity model and a 3-D fault geometry. The convolution of the Green's function and a triangle function produces synthetic seismic waveforms for each subfault to every station. Triangle function controls the rise time of slip on each subfault. I take the 2020 Samos earthquake (37.90°N, 26.82°E), Turkey as an example to generate synthetic waveforms (Figure 1).

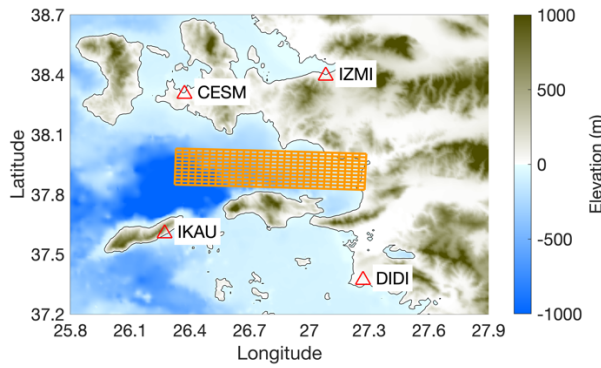


Figure 1. The region and fault model of seismic simulation. Orange mesh represents the fault model of the Samos earthquake; red triangles represent the recording stations. The strike and dip of the fault model are 272° and 48°, respectively. The number of subfault is 280 (strike direction: 28; dip direction: 10). The length and width of each subfault are 3 km.

According to convolution theory, the convolution of Green's function ($G(t)$) and a triangle function ($T(t)$) is equal to multiply them in frequency domain.

$$\mathcal{F}\{G(t) * T(t)\} = \mathcal{F}\{G(t)\}\mathcal{F}\{T(t)\} \quad (1)$$

With changing the width of triangle function, synthetic waveform with different rise times can be calculated. Triangle function in frequency domain is a sinc function whose width shrinks with rise time increase. Considering this feature of triangle function in frequency domain, I modify the equation

$$\mathcal{F}\{G(t) * T_n(t)\} = \mathcal{F}\{G(t)\}\mathcal{F}\{T_n(t)\} = \mathcal{F}\{G(t)\}\mathcal{F}\{T_1(t)\}\mathcal{F}\{f(t)\} \quad (2)$$

where T_n is triangle function and the rise time is n ; T_1 is the basis triangle function (rise time = 1 sec and slip value = 1 meter); $f(t)$ is a filter function. $\mathcal{F}\{T_n(t)\}$ is equal to $\mathcal{F}\{T_1(t)\}\mathcal{F}\{f(t)\}$. A suitable filter reshapes the basis triangle function to match certain rise time functions (Fig. 2). Then, the filtered synthetic waveform can be gained by inverse Fourier Transform. In theory, the filtered synthetic waveforms will be equal to the results of forward simulation because they share the same spectrum pattern. For testing this hypothesis, I use rise times of 1, 2, 3 and 5 sec, and take rise time of 1 sec as a basis function. The rests are test targets, and their forward results are used to validate my work. In addition, I simply adopt Gaussian function as filter functions. To quantify the errors of waveform matching, I adopt root mean square error (RMS) as a measurement.

$$RMS = \sqrt{\frac{\sum (w_s - w_f)^2}{n}} \quad (3)$$

where, w_s is the waveforms from forward simulation; w_f is the waveforms from filter method; n is the number of time series ($n=480$). I use 512 points and $dt=0.2$ sec to do seismic simulation.

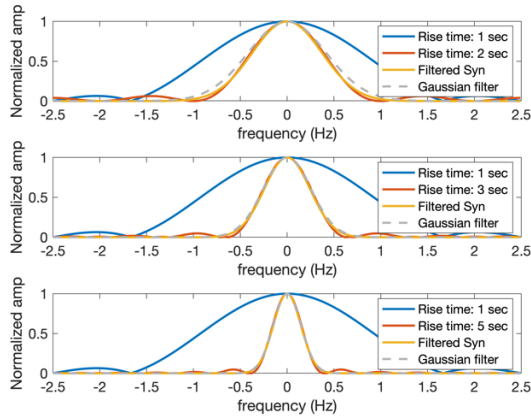


Figure 2. This figure shows Gaussian filters reshape the basis triangle functions (1 sec) to the target functions of certain rise times (2, 3 and 5 seconds).

Results

Using Gaussian function as a filter reshapes the spectrum of the basis function tuning it into a corresponding rise time. Figure 2 shows the filtered spectrums with different rise times are match the target spectrum patterns. All central parts, the big structures, fit well. However, because triangle function in frequency domain is a sinc function, the Gaussian filter cannot deal with the ripple tails at higher frequency. This feature of different shapes causes some issues we will discuss later.

With inverse Fourier Transform, the filtered synthetic waveforms can be produced, and the consequences of using filter can be remove by tapping and phase shifting depending on the filter design. Figure 3 shows the results of inverse Fourier Transform of filtered spectrums. All waveforms match perfectly as well, and only at the peak places and turning points have slight misses.

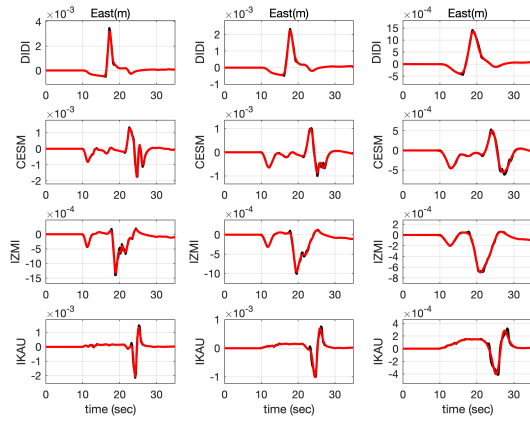


Figure 3. The forward and filtered synthetic waveforms at east component generated by the first subfault. The waveforms from left to right are rise time results of 2, 3 and 5 seconds, respectively. Black lines are the results of forward simulations; red lines are the results of filtered synthetic waveforms.

Figure 4 shows the statistical results of RMS including all results from all subfault to every station. Compared to the scales of waveform values, the errors are significant small. The most errors are under 2×10^{-5} . The most errors of rise time of 2 sec are at $1-2 \times 10^{-5}$, the second bin, and for the rise times of 3 and 5 seconds, the numbers of errors decay with the RMS value increase.

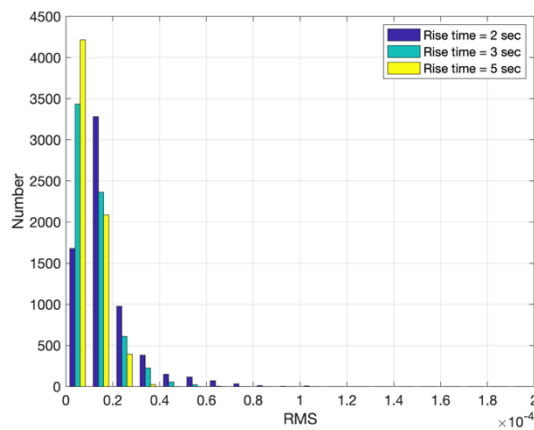


Figure 4. The RMS histogram of different rise times.

Discussion

Figure 3 shows the filtered synthetic waveforms at peaks and turning points cannot match very well. Moreover, compared with the simulated waveforms, the filtered synthetic waveforms are smoother. This is because using the simple Gaussian filters cannot perfectly deal with the ripple tails of triangle functions. However, it does not mean using Gaussian filters is wrong. The reason is that triangle function in fact contributes the ripples, artificial energy, at high frequency so these high frequency signals would not be real in time domain. Another reason is that the resolution of simulation depends on how fine velocity structure and fault models are used (Lee et al., 2015). In my case, I only use 1-D layered velocity structure without considering topography and near-ground velocity model, so the resolution won't reach high frequency, even if my Δt is 0.2 sec. Therefore, the misses in my approach can be ignored. Furthermore, the patterns of RMS distributions also imply this spectrum effect by the Gaussian filters. The rise time of 2 sec has relatively large errors because there is more missed matching at higher frequency. With increase of rise time, the errors concentrate toward the first bin, and rise time of 5 sec has the highest number of RMS at the first bin. The change of RMS distribution is dynamic, which is with rise time change. However, this phenomenon is under my approach causing the high frequency issue. If there is a filter that can perfectly reshape the rise time function or there is a rise time function that can fit the Gaussian filter, there will be no error.

All seismic simulations use 4 CPU cores of Intel Core i5 with 2.3 GHz and calculate seismic waveforms from 280 subfaults to 4 recording stations. The difference is that the synthetic simulation is based on python, but the filtered simulation is based on MATLAB. In the average of 5 simulations, the original seismic simulation takes 14.41 sec, and the filtered simulation takes 13.18 sec in parallel calculation. After optimization following the feature of matrix calculation in MATLAB, it takes 12.29 sec. If the storage space of matrix is already opened (it does not mean pre-load the basis functions), the filtered approach takes 10.11 sec and it under matrix feature is 7.49 sec. Although it is obvious to see the filtered approach is faster than original one, it still needs more tests to gain a robust result, especially under the same language.

Conclusions

I use the Gaussian filters to reshape the spectrum patterns of the basis synthetic functions to match the target rise time functions. I set rise time of 1 sec as a basis

function and use the simulated results of 2, 3 and 5 seconds to validate my approach. The results show this approach is doable and the errors can be ignored because of the rise time function and the frequency resolution of the simulation model. They also show the computing time is significantly reduced. By this approach, it only needs one simulation and then others with lower rise time frequency can be generated by filter processing. This filtered seismic simulation increases the flexibility of changing rise time function and saves more computing time.

References

- Lee, S. J., Chen, H. W., Liu, Q., Komatitsch, D., Huang, B. S., & Tromp, J. (2008). Three-dimensional simulations of seismic-wave propagation in the Taipei basin with realistic topography based upon the spectral-element method. *Bulletin of the Seismological Society of America*, 98(1), 253-264.
- Lee, S. J., Chan, Y. C., Komatitsch, D., Huang, B. S., & Tromp, J. (2009). Effects of realistic surface topography on seismic ground motion in the Yangminshan region of Taiwan based upon the spectral-element method and LiDAR DTM. *Bulletin of the Seismological Society of America*, 99(2A), 681-693.
- Lee, S. J. (2015) Numerical earthquake model of the 20 April 2015 southern Ryukyu subduction zone M6.4 event and its impact on seismic hazard assessment. *Earth Planet Space*, 67, 164. <https://doi.org/10.1186/s40623-015-0337-5>
- Lee, Y. T., K. F. Ma, M. C. Hsieh, Y. T. Yen, & Y. S. Sun, 2016: Synthetic ground-motion simulation using a spatial stochastic model with slip self-similarity: Toward near-source ground-motion validation. *Terrestrial, Atmospheric and Oceanic Sciences*, 27, 397-405, doi: 10.3319/TAO.2015.11.27.01(TEM)
- Melgar, D., and Y. Bock (2015), Kinematic earthquake source inversion and tsunami runup prediction with regional geophysical data, *Journal of Geophysical Research*, Solid Earth, 120, 3324–3349, doi:10.1002/2014JB011832.
- Melgar, D., & Hayes, G. P. (2017). Systematic observations of the slippulse properties of large earthquake ruptures. *Geophysical Research Letters*, 44, 9691–9698. <https://doi.org/10.1002/2017GL074916>
- Kubo, H., Suzuki, W., Aoi, S., & Sekiguchi, H. (2017) Source rupture process of the 2016 central Tottori, Japan, earthquake (M JMA 6.6) inferred from strong motion waveforms. *Earth Planets Space*, 69, 127. <https://doi.org/10.1186/s40623-017-0714-3>